



Mapping gains and losses in woody vegetation across global tropical drylands

Tian, Feng; Brandt, Martin Stefan; Liu, Yi Y; Rasmussen, Kjeld; Fensholt, Rasmus

Published in:
Global Change Biology

DOI:
[10.1111/gcb.13464](https://doi.org/10.1111/gcb.13464)

Publication date:
2017

Document version
Peer reviewed version

Citation for published version (APA):
Tian, F., Brandt, M. S., Liu, Y. Y., Rasmussen, K., & Fensholt, R. (2017). Mapping gains and losses in woody vegetation across global tropical drylands. *Global Change Biology*, 23(4), 1748-1760.
<https://doi.org/10.1111/gcb.13464>

1 **Title:** Mapping gains and losses in woody vegetation across global tropical drylands

2 **Running head:** Gains and losses in dryland woody vegetation

3 **Authors:** Feng Tian¹, Martin Brandt¹, Yi Y. Liu², Kjeld Rasmussen¹, Rasmus Fensholt¹

4 ¹ Department of Geosciences and Natural Resource Management, University of Copenhagen,
5 1350 Copenhagen, Denmark

6 ² ARC Centre of Excellence for Climate Systems Science & Climate Change Research
7 Centre, University of New South Wales, Sydney, Australia

8 **Corresponding author:** Feng Tian, Telephone: +45 35334738, emails: feng.tian@ign.ku.dk;
9 ftian2012@gmail.com

10 **Keywords:** Trend analysis, non-photosynthetic woody component, drylands, woody
11 vegetation, shrub encroachment, deforestation, remote sensing.

12 **Type of Paper:** Technical Advance

13

14 **Abstract**

15 Woody vegetation in global tropical drylands is of significant importance for both the inter-
16 annual variability of the carbon cycle and local livelihoods. Satellite observations over the
17 past decades provide a unique way to assess the vegetation long-term dynamics across biomes
18 worldwide. Yet, the actual changes in the woody vegetation are always hidden by inter-
19 annual fluctuations of the leaf density, because the most widely used remote sensing data are
20 primarily related to the photosynthetically active vegetation components. Here, we quantify
21 the temporal trends of the non-photosynthetic woody components (i.e. stems and branches) in
22 global tropical drylands during 2000-2012 using the vegetation optical depth (VOD),

23 retrieved from passive microwave observations. This is achieved by a novel method focusing
24 on the dry season period to minimize the influence of herbaceous vegetation, and using
25 MODIS (MODerate resolution Imaging Spectroradiometer) NDVI (Normalized Difference
26 Vegetation Index) data to remove the inter-annual fluctuation of the woody leaf component.
27 We revealed significant trends ($p < 0.05$) in the woody component (VOD_{wood}) in 35% of the
28 areas characterized by a non-significant NDVI trend, indicating pronounced gradual
29 growth/decline in woody vegetation not captured by traditional assessments. The method is
30 validated using a unique record of ground measurements from the semi-arid Sahel and shows
31 a strong agreement between changes in VOD_{wood} and changes in ground observed woody
32 cover ($r^2 = 0.78$). Reliability of the obtained woody component trends is also supported by a
33 review of relevant literatures for eight hot-spot regions of change. The proposed approach is
34 expected to contribute to an improved assessment of e.g. changes in dryland carbon pools.

35

36 **Introduction**

37 While vegetation in drylands has relatively low biomass, as compared to the humid areas, it is
38 of significant importance for several reasons: Firstly, drylands cover approximately 41% of
39 the Earth's terrestrial surface, and therefore total biomass and carbon stock of vegetation in
40 drylands are still a substantial part of the global total (IPCC, 2014). Secondly, the variability
41 of vegetation in drylands is comparatively high, implying that short-term changes in global
42 carbon stocks may be dominated by the contribution from drylands (Ahlstrom *et al.*, 2015,
43 Liu *et al.*, 2015). Thirdly, vegetation in drylands provides both products and services of great
44 importance for local livelihoods (Adeel *et al.*, 2005). Trend analysis of long-term Earth
45 Observation (EO) data has been widely used as means to assess vegetation dynamics in
46 drylands (Fensholt *et al.*, 2012, Horion *et al.*, 2016). Moreover, different vegetation functional
47 types (i.e. persistent vegetation and recurrent vegetation) have been assessed separately in

48 order to gain insights of the vegetation changes and its relation to changes in climate and
49 human activities (Andela *et al.*, 2013, Archibald & Scholes, 2007, Donohue *et al.*, 2009,
50 Fensholt *et al.*, 2015). Specifically, herbaceous vegetation is characterized by a short life-span
51 (months or years) and large inter-annual variability driven by water availability and
52 ecological disturbances (e.g. fires), whereas woody plants are characterized by a longer life-
53 span (decades or centuries) with more stable growth conditions, particularly for the woody
54 component (i.e. stems and branches).

55 Relatively few global scale quantitative studies on changes in dryland woody vegetation are
56 available. Most researches on global deforestation/forest change are not designed to map
57 woody vegetation in drylands, since they often do not fulfill the criteria of ‘forest’ (e.g. the
58 FAO criterion of 10% crown cover, an area of more than 0.5 hectares and tree height above 5
59 m) (Hansen *et al.*, 2013, Shimada *et al.*, 2014). The few studies focusing on woody vegetation
60 trends in drylands at regional scale used the normalized difference vegetation index (NDVI)
61 data from optical sensors, e.g. MODerate resolution Imaging Spectroradiometer (MODIS)
62 that are highly sensitive to the photosynthetic leaf component and largely insensitive to the
63 non-photosynthetic woody component (Brandt *et al.*, 2016a, Horion *et al.*, 2014, Mitchard &
64 Flintrop, 2013).

65 The leaf component is generally only a small fraction of the entire above-ground woody
66 biomass, and may not be representative of the trends and spatial patterns of the woody
67 component. In drylands the leaf component is often strongly related to water availability, and
68 may therefore change quite rapidly depending on inter-annual variations in rainfall. Also, the
69 spatial variability of soil conditions and topography partly control water availability.
70 Moreover, large differences in phenology are found between woody species and consequently
71 changes in species composition will result in substantial changes in the leaf component

72 (Brandt *et al.*, 2016b) that are not necessarily reflected in changes in woody biomass. In
73 addition, fires will have a considerable impact on inter-annual variations of leaf density and
74 mass. All these factors will cause inter-annual fluctuations of the leaf component and tend to
75 mask the supposedly more gradual and continuous trends in woody biomass.

76 Microwave sensor observations are sensitive to the water content in both photosynthetic
77 (herbaceous and woody plant leaves) and non-photosynthetic (woody stems and branches)
78 vegetation components (Jones *et al.*, 2013). The contribution of each component to the
79 observed signals highly depends on the microwave frequency used. Observations from low
80 frequency (i.e. 1.4 GHz) carry information mainly on the woody component (more related to
81 branches for forests), while the relative information on the leaf component increases
82 significantly with higher frequencies (Ferrazzoli *et al.*, 2002, Guglielmetti *et al.*, 2007, Santi
83 *et al.*, 2009). The L-band (1-2 GHz) radar backscatter has been shown to be highly correlated
84 to woody biomass in tropical savannas and woodlands (Mitchard *et al.*, 2009). Yet, available
85 L-band radar data have a limited record length hampering woody vegetation change studies
86 spanning decades, and it is still challenging to apply radar backscatter data for woody biomass
87 estimation at regional to global scales due to the difficulties of accounting for spatial
88 variability in soil properties and vegetation geometrical distributions at a high spatial
89 resolution (Kerr, 2007).

90 Recently, Liu *et al.* (2011) produced a global long-term vegetation optical depth (VOD)
91 dataset retrieved from satellite passive microwave radiometer observations at frequencies
92 higher than 6.8 GHz, which was shown to carry important information on woody vegetation
93 yet heavily influenced by the herbaceous vegetation and woody plant leaves (Grant *et al.*,
94 2016, Tian *et al.*, 2016). In this study, we present a method to separate the leaf and woody
95 components by the combined use of VOD and NDVI datasets to obtain a more accurate

96 assessment of woody vegetation changes/trends in global tropical drylands for the period
97 2000 to 2012.

98

99 **Materials and methods**

100 ***Study area***

101 According to the UNEP (United Nations Environment Program) humidity map, global
102 drylands are defined to include hyper-arid, arid, semi-arid and dry-subhumid regions. In this
103 study, we focused on the tropical (between 35°N and 35°S) dryland areas, including the
104 majority of woody vegetation of global drylands. Annual rainfall is usually below 800 mm
105 and concentrated in the wet/growing season, with high inter-annual variability in both rainfall
106 amount and timing (Adeel *et al.*, 2005). The typical vegetation in tropical drylands are annual
107 herbaceous plants, shrubs and trees with open canopy cover, classified as savanna, shrublands
108 or woodland depending on the dominant plant types. Annual herbaceous vegetation normally
109 completes their life cycle during a single growing season spanning few months, governed by
110 the timing of the rainy season. Contrastingly, trees and shrubs may show distinctly different
111 seasonal cycles dependent on the species, i.e. evergreen, semi-evergreen or deciduous.

112 ***NDVI and VOD data***

113 We used the Collection 6 Terra MODIS monthly product MOD13C2 with a spatial resolution
114 of 0.05 degree (about 5.5 km at equator) and covering from 2000 to present (Didan, 2015).
115 The surface reflectance bands have been corrected for atmospheric effects (Vermote &
116 Kotchenova, 2008) and sensor degradation (Detsch *et al.*, 2016, Lyapustin *et al.*, 2014). To
117 match the spatial resolution of VOD data, the red and near-infrared reflectance bands were
118 aggregated to 0.25 degree by averaging before calculation of NDVI data.

119 The VOD data retrieval is based on the Land Parameter Retrieval Model (LPRM) (Owe *et al.*,
120 2001) with inputs of satellite passive microwave observations from several sensors, including
121 the Special Sensor Microwave Imager (SSM/I), the Advanced Microwave Scanning
122 Radiometer – Earth Observing System (AMSR-E), the WindSat and the FengYun-3B (Liu *et*
123 *al.*, 2015). The microwave frequency of each sensor used is 19.4 GHz, 6.9 GHz, 6.8 GHz and
124 10 GHz, respectively. A cumulative distribution function (CDF) matching approach was used
125 to merge the VOD retrievals from different sensors without changing the inter-annual
126 variations and long-term trends (Liu *et al.*, 2012). The VOD dataset was produced at a
127 monthly temporal interval from 1988 to 2012 and a spatial resolution of 0.25 degree (about 27
128 km at equator). The data is consistent among sensors as evaluated in Tian *et al.* (2016).

129 ***Conceptual design***

130 The VOD retrievals from microwave emission at frequencies higher than 6.8 GHz are related
131 to the water content in both the herbaceous plants and the woody plant leaves/stems/branches
132 (Guglielmetti *et al.*, 2007, Santi *et al.*, 2009). In drylands characterized by a long dry season,
133 the contribution from herbaceous vegetation will rapidly disappear and become negligible a
134 few months into the dry season, and consequently the signal from woody vegetation will
135 dominate. In order to separate the contributions from the leaf and woody components, we
136 employed the independent information from MODIS NDVI which represents the amount of
137 photosynthetically active plant material, and is largely determined by green leaves (i.e. leaf
138 density) of woody vegetation in the dry season (Brandt *et al.*, 2016b). The overall conceptual
139 design is shown in Fig. 1a and the detailed procedure of retrieving trends/changes in the
140 woody component is described as follows (illustrated in supplementary material Fig. S1 based
141 on simulated data):

142 i. For each pixel over a certain period of years, we decompose the observed dry season
 143 VOD (denoted as VOD_{raw}) and the corresponding observed NDVI signal (denoted as
 144 $NDVI_{\text{raw}}$) into two components: the long-term trend (LTT) and the inter-annual
 145 variations (IAV), respectively:

$$146 \quad VOD_{\text{raw}} = VOD_{\text{LTT}} + \Delta VOD_{\text{IAV}} \quad (1)$$

$$147 \quad NDVI_{\text{raw}} = NDVI_{\text{LTT}} + \Delta NDVI_{\text{IAV}} \quad (2)$$

148 Both the leaf and woody components would contribute to VOD_{LTT} and VOD_{IAV} , while
 149 the $NDVI_{\text{LTT}}$ and $NDVI_{\text{IAV}}$ are primarily attributed to the leaf component.

150 ii. If there is a significant correlation between VOD_{IAV} and $NDVI_{\text{IAV}}$, we assume that the
 151 VOD_{IAV} is dominated by a contribution from the leaf component while the woody
 152 component is relatively stable over time. Then we establish a linear regression
 153 between VOD_{IAV} and $NDVI_{\text{IAV}}$:

$$154 \quad \Delta VOD_{\text{IAV}} = \beta \times \Delta NDVI_{\text{IAV}} + \varepsilon \quad (3)$$

155 Where β and ε are the slope and the residuals, respectively, varying as a function of
 156 woody vegetation density and species composition. Note that the intercept of the
 157 regression is 0 since both the independent and response variables have been already
 158 detrended. We built the regression model using the detrended VOD/NDVI instead of
 159 the original VOD/NDVI observations to avoid an underestimation of the trend in the
 160 woody component (Supplementary material Fig. S1).

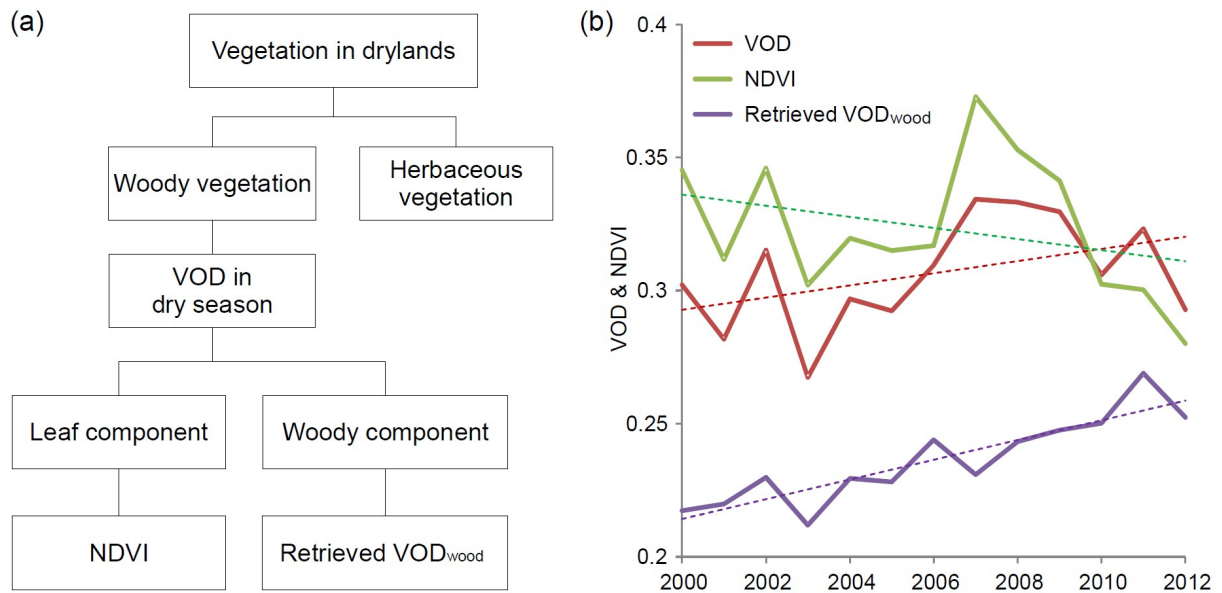
161 iii. We apply the slope parameter (β) to $NDVI_{\text{raw}}$ to estimate the contribution from the leaf
 162 component to both VOD_{LTT} and VOD_{IAV} (denoted as VOD_{leaf}):

$$163 \quad VOD_{\text{leaf}} = \beta \times NDVI_{\text{raw}} + b \quad (4)$$

164 Then the difference between VOD_{raw} and the estimated VOD_{leaf} would be the
 165 contribution from the woody component (denoted as VOD_{wood}):

166
$$\text{VOD}_{\text{wood}} = \text{VOD}_{\text{raw}} - \text{VOD}_{\text{leaf}} \quad (5)$$

167 It must be noted that we focus only on the long-term trends in VOD_{wood} , as the
 168 absolute values of VOD_{wood} cannot be obtained with the lack of estimation of b in
 169 equation (4).



170
 171 **Fig. 1** (a) Conceptual design of the estimation of trends in the dryland woody vegetation component.
 172 (b) An example pixel (9.5°N, 18.75°E) showing the temporal profile of NDVI, VOD and the retrieved
 173 VOD_{wood} . Note that the focus of this approach is on the temporal trend of the retrieved VOD_{wood} , since
 174 the absolute values cannot be inferred.

175 ***Applying to remote sensing data***

176 The method proposed was applied to monthly MODIS NDVI and VOD data from 2000 to
 177 2012 being the intersection period of the NDVI and VOD datasets used. The VOD and NDVI
 178 data were detrended per pixel to obtain the inter-annual variation VOD_{IVA} and NDVI_{IAV} ,
 179 respectively. Pixels with a non-significant t ($p \geq 0.05$) linear correlation between VOD_{IVA} and
 180 NDVI_{IAV} were masked out for retrieval of VOD_{wood} , and also pixels with an NDVI value
 181 below 0.1 were excluded in the analysis to minimize influences from the soil background

182 (Huete, 1988). We determined the dry season period as the three months with lowest values in
183 each dry season of the VOD observations (accounting for cross calendar-year minimum of
184 VOD values in the southern hemisphere). To reduce the impact of cloud cover, we compared
185 the Pearson product-moment correlation coefficient between all the seven possible
186 combinations within the three months of detrended VOD and NDVI (i.e. first minimum,
187 second minimum, third minimum, average of first and second minimum, average of first and
188 third minimum, average of second and third minimum, and average of all the three months)
189 and selected the one characterized by the highest r value. An example shows that the retrieved
190 VOD_{wood} is more stable over time as compared to both NDVI and VOD (Fig. 1b). The NDVI
191 trend was transformed into VOD units by multiplying the slope value β to be comparable with
192 the retrieved VOD_{wood} trend.

193 *Validation with in situ measurements*

194 Time series data of *in situ* woody cover and leaf biomass available from Senegal were used to
195 validate the retrieved trends of the woody and leaf components, respectively. Validating long-
196 term trends requires continuous field data records covering a long time period and being
197 representative for areas comparable with the spatial resolution of the satellite data. Moreover,
198 *in situ* data should ideally include a broad range of ecosystem functional types and be located
199 in areas where actual trends are observed. This study uses a unique data set of 11 ground sites
200 (supplementary Fig. S2), located along a north-south rainfall gradient in Senegal (200-800
201 mm/year) covering the full time period of this study. The woody plant cover along this
202 gradient increases from approximately 3% in the north to more than 40% in the south,
203 including typical dryland evergreen and deciduous species (Brandt *et al.*, 2016b). Moreover,
204 significant changes within the last 15 years are observed in these areas (Brandt *et al.*, 2015).
205 Each site consists of a 1 km transect line, and the canopy cover of all woody plants

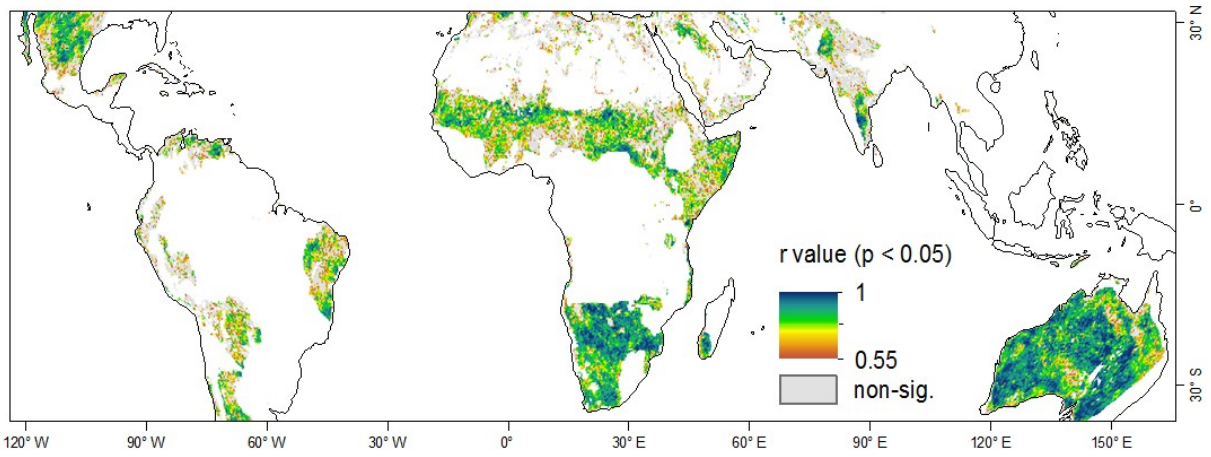
206 (regardless of size) was measured every two years in 4 circular plots, spaced at 200 m
207 intervals (Brandt *et al.*, 2016b). Furthermore, the leaf biomass of woody species was
208 investigated for the same sites using allometric models (Diouf *et al.*, 2015). Leaf mass and
209 density is closely related to inter-annual rainfall variations, whereas the woody cover is more
210 stable and representative for the woody vegetation density.

211 The scale differences between the *in situ* measurements and satellite data inevitably introduce
212 bias since pixel values generally tend to over/under estimate lowest/highest plot scale values
213 (Fensholt *et al.*, 2006). However, the sites are originally selected to be representative for
214 relatively large homogeneous areas (Diallo *et al.*, 1991) and have been successfully linked
215 with VOD pixels (Tian *et al.*, 2016). Therefore, it was deemed feasible in this case to perform
216 pixel vs. plot scale comparisons between the trends of EO data and *in situ* measurements.

217 **Results**

218 ***Trends in different woody vegetation components***

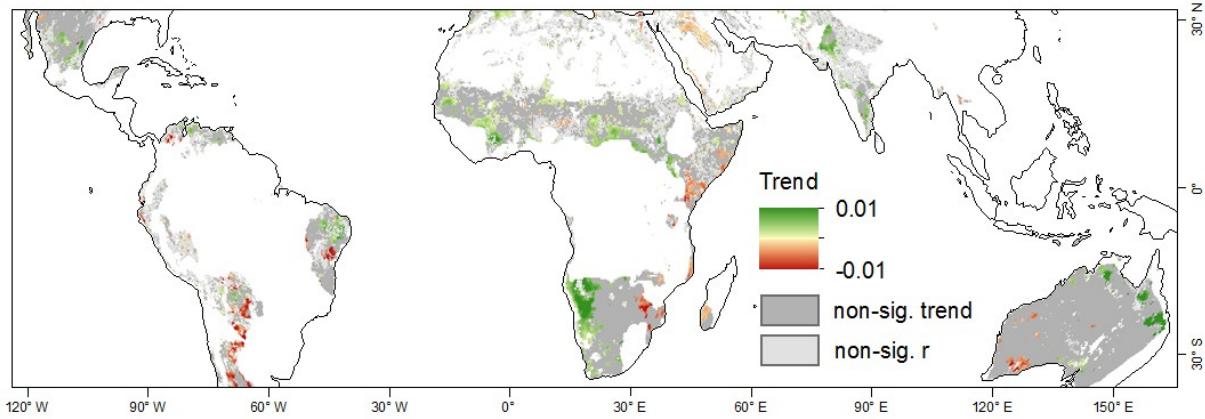
219 The detrended dry season VOD data is significantly ($p < 0.05$) correlated with the
220 corresponding detrended NDVI data in 71% of global tropical drylands over the period 2000-
221 2012 (Fig. 2). For these areas, 14% of the NDVI pixels show significant trends ($p < 0.05$,
222 located mainly in southern Africa and Australia, Fig. 3b), while 27% of the VOD pixels have
223 significant trends (Fig. 3a). After removing the leaf inter-annual fluctuation from the VOD
224 signal, the retrieved VOD_{wood} shows significant trends in 36% of global tropical drylands (Fig.
225 3c). Furthermore, for pixels with a non-significant NDVI trend, 35% show a significant
226 VOD_{wood} trend (22% positive and 13% negative), revealing considerable areas characterized
227 by a woody vegetation trend obscured by leaf fluctuations (Fig. 4).



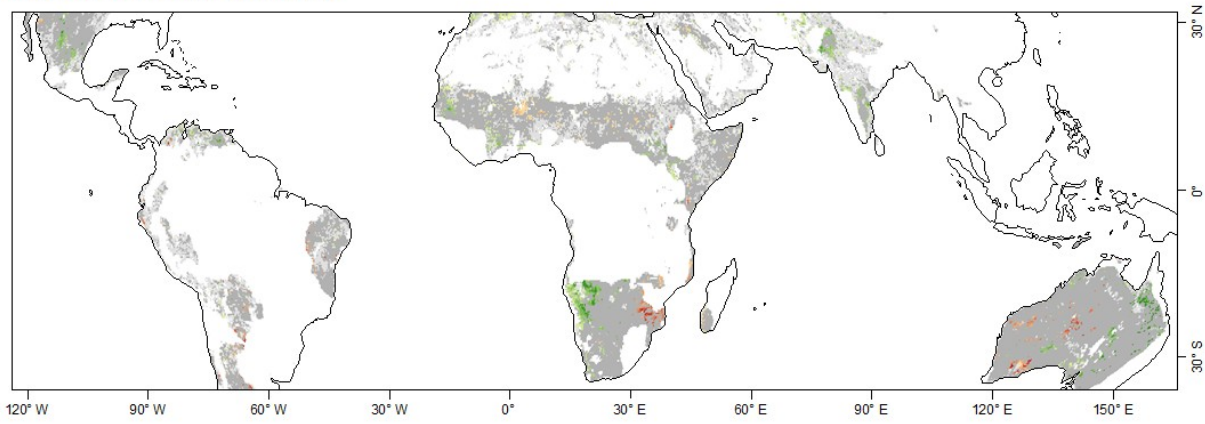
228

229 **Fig. 2** Correlation coefficients (r value) between detrended NDVI and detrended VOD time
230 series during 2000-2012.

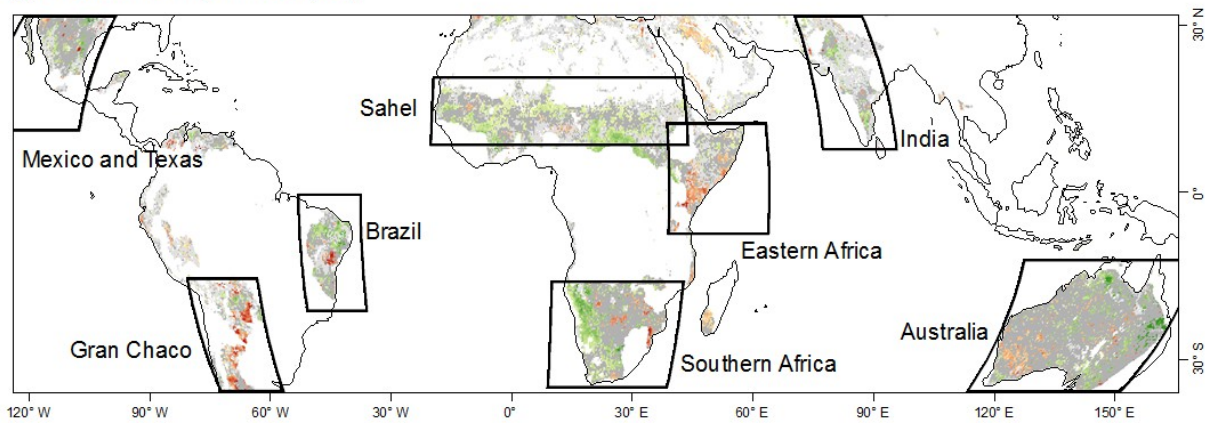
(a) VOD trend



(b) NDVI trend (unit: VOD/year)

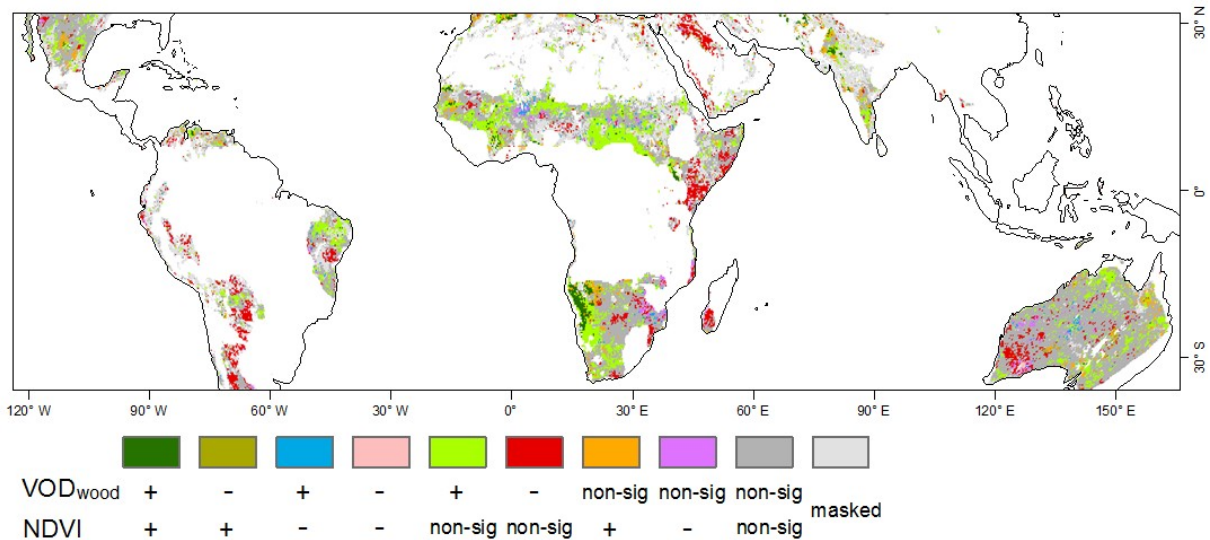


(c) VOD_{wood} trend (unit: VOD/year)



231

232 **Fig. 3** Trends of (a) VOD, (b) NDVI, and (c) VOD_{wood} during 2000-2012. Pixels with non-
233 significant ($p \geq 0.05$) correlation between detrended NDVI and detrended VOD are masked
234 with light grey color. Pixels with non-significant trends ($p \geq 0.05$) are masked with dark grey
235 color. Black boxes in (c) delineate hot-spot areas of VOD_{wood} changes (Fig. 6).

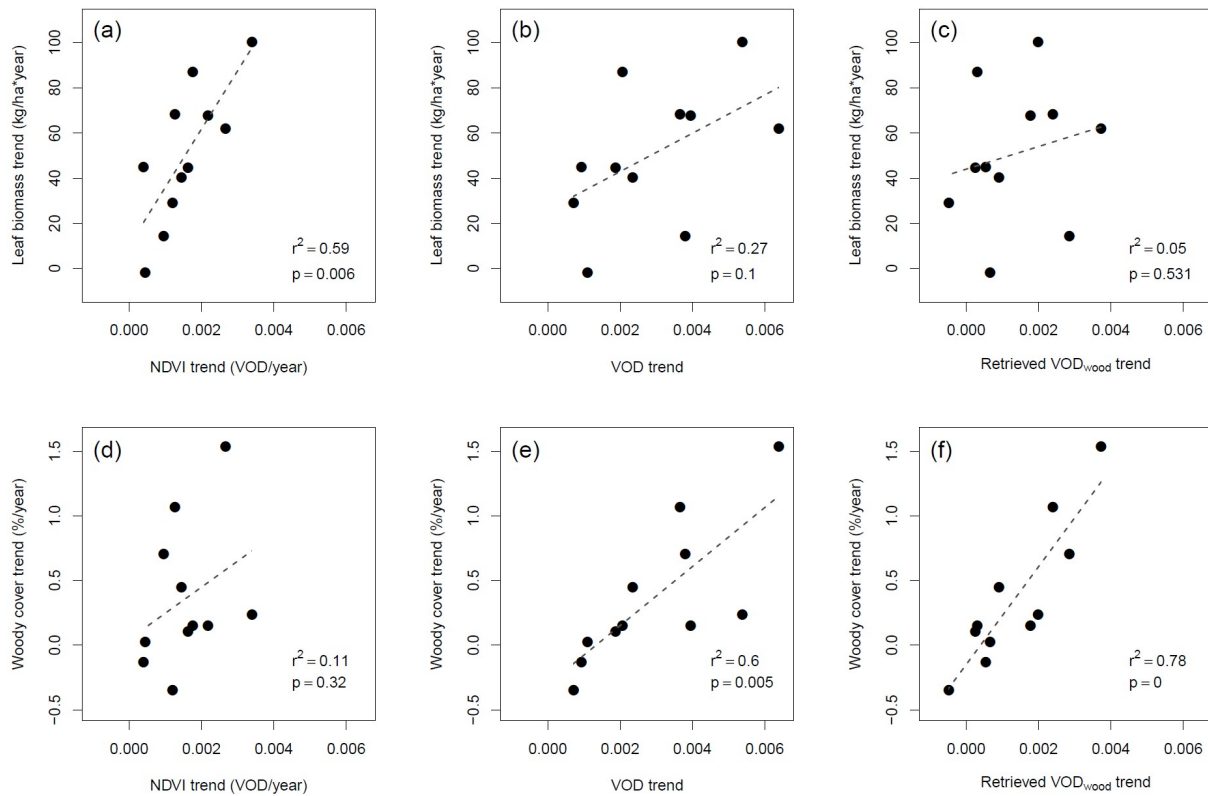


236

237 **Fig. 4** Spatial patterns of different trend combinations of VOD_{wood} (woody component) and
 238 NDVI (leaf component).

239 ***Validation with in situ measurements***

240 The NDVI derived leaf trend is strongly coupled to the *in situ* leaf biomass trend ($r^2 = 0.59$; p
 241 < 0.01 , Fig. 5a), yet not significantly correlated with the *in situ* woody cover trend (Fig. 5c).
 242 Contrastingly, the VOD_{wood} trend is highly correlated with the *in situ* woody cover trend ($r^2 =$
 243 0.78 ; $p < 0.001$, Fig. 5f) whereas no significant correlation with the *in situ* leaf biomass trend
 244 is observed (Fig. 5d). The VOD trend shows an intermediate correlation with both the *in situ*
 245 leaf biomass trend ($r^2 = 0.27$; $p < 0.1$, Fig. 5b) and the *in situ* woody cover trend ($r^2 = 0.60$; p
 246 < 0.01 , Fig. 5e). Therefore, the method based on the complementary information in the VOD
 247 and NDVI datasets has proven to successfully reduce the inter-annual fluctuations of the
 248 VOD signal associated with the leaf component, thereby representing the woody vegetation
 249 trend better than when using only VOD.

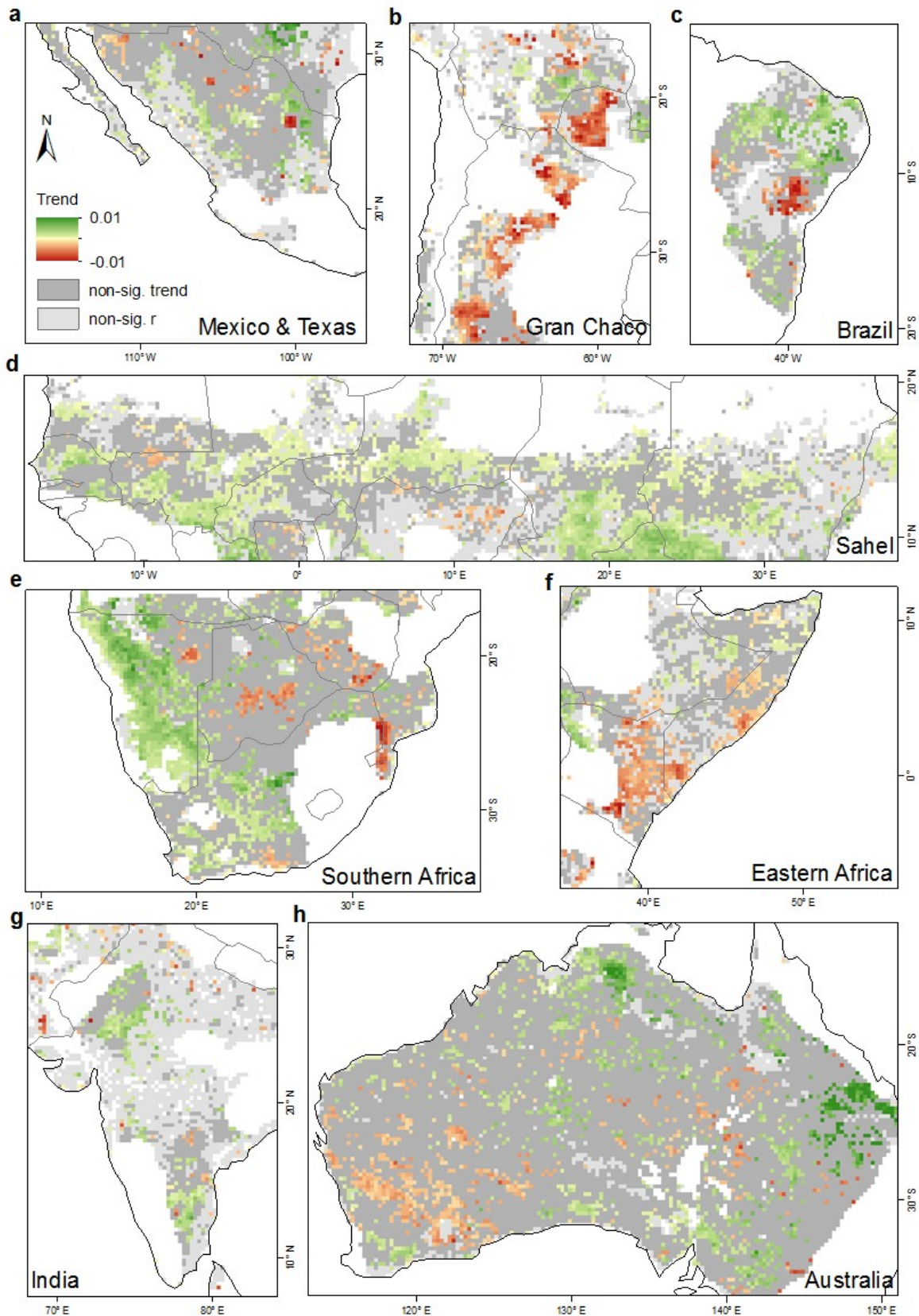


250

251 **Fig. 5** Relationships between trends of *in situ* measured (a-c) leaf biomass and (d-f) woody
 252 canopy cover and trends of (a, d) NDVI, (b, e) VOD, and (c, f) VOD_{wood} . Locations and
 253 measurements of all *in situ* sites are shown in supplementary Fig. S2 and S3.

254 ***Sub-continental hot-spot regions of change***

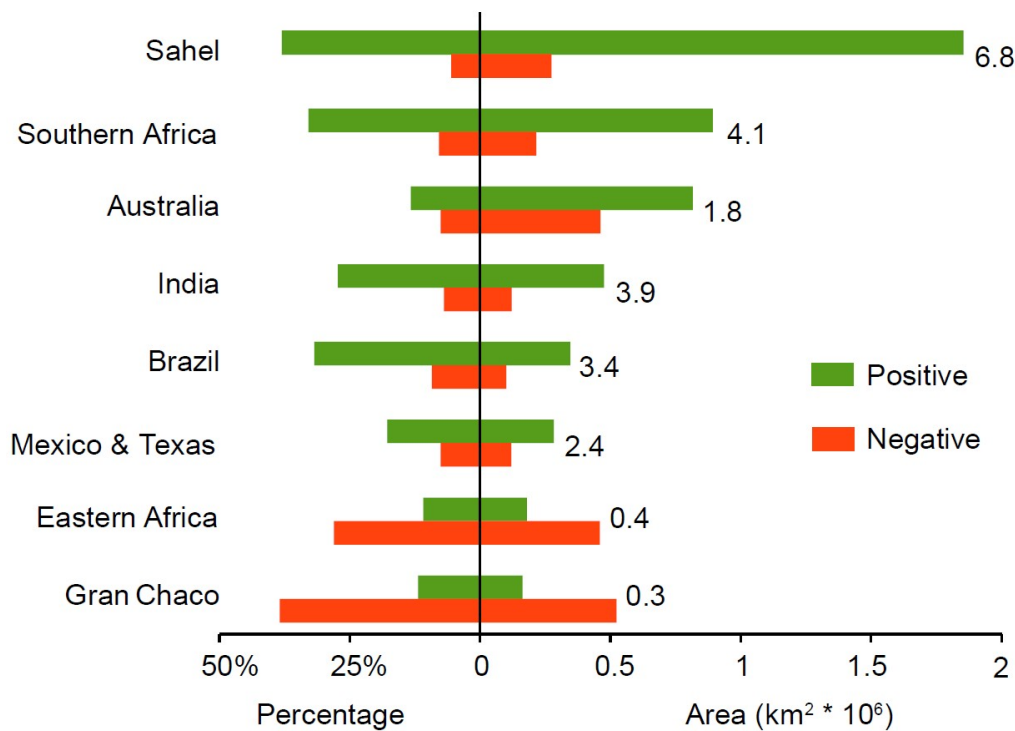
255 During the period 2000-2012, the trends in VOD_{wood} were found to be significantly ($p < 0.05$)
 256 positive in 22.7% of global tropical drylands whereas 13.3% were characterized by a
 257 significantly negative trend. We selected eight sub-continental hot-spot change regions of
 258 VOD_{wood} trends for further analyses (as indicated in Fig. 3c and enlarged in Fig. 6). The total
 259 area of significant VOD_{wood} trends and the percentage of significant trends per area for each
 260 hot-spot change region are summarized in Fig. 7. Large coherent areas of pronounced
 261 increasing VOD_{wood} trends are observed in Sahel, Namibia and South Africa, and East
 262 Australia. Contrastingly, areas of significant decreasing VOD_{wood} trends are found in Gran
 263 Chaco, eastern Africa, West Australia, and the eastern part of southern Africa.



264

265 **Fig. 6** Trends of VOD_{wood} in hot-spot change regions of (a) Mexico & Texas, (b) Gran Chaco,
 266 (c) Brazil, (d) Sahel, (e) southern Africa, (f) eastern Africa, (g) India, and (h) Australia.

267 Spatial extend of hot-spot change regions is indicated by the black boxes in Fig. 3c. Pixels
 268 with a non-significant ($p \geq 0.05$) correlation between detrended NDVI and detrended VOD
 269 are masked with light grey color. Pixels with non-significant trends ($p \geq 0.05$) are masked
 270 with dark grey color.



271
 272 **Fig. 7** Area (km²*10⁶) and percentages of significant ($p < 0.05$) positive and negative
 273 VOD_{wood} trends for the sub-continental hot-spot regions of change (Fig. 6). The ratio between
 274 areas of positive and negative trends is given by the number on the right side of each bar.

275 **Discussion**

276 ***Trends in woody vegetation***

277 This study attained a separation between trends of the leaf and woody components in global
 278 tropical drylands (2000-2012) by combing satellite observations from optical and passive
 279 microwave sensors. By removing the inter-annual fluctuations and trends of the leaf
 280 component, we revealed regional scale trend patterns in woody vegetation which have not

281 been shown previously. In addition, we found areas characterized by diverging trends in the
282 retrieved VOD_{wood} and NDVI data. This can be related to changes in composition of trees and
283 shrubs within the footprint (~ 25 km) of a VOD pixel since trees and shrubs are characterized
284 by different signatures in the proportion of leaf and woody components (Andela *et al.*, 2013).
285 Given a similar amount of the woody component, shrubs generally look greener (higher
286 NDVI) than trees as shrubs in this case will have a higher fractional vegetation cover. For
287 example, Herrmann and Tappan (2013) reported an impoverishment of trees and
288 encroachment of shrubs between the early 1980s and 2010 in central Senegal despite a
289 positive NDVI trend. This area corresponds with the pixels with a non-significant VOD_{wood}
290 trend and significant positive NDVI trend (colored as orange) in Fig. 4.

291 Quantifying trends/changes in different vegetation components remains a challenge for state-
292 of-the-art dynamic global vegetation models (DGVMs) due to the complex responses of
293 biomass partitioning process to plant type and size, nutrient supply and climate at global scale
294 (De Kauwe *et al.*, 2014, Piao *et al.*, 2013, Poorter *et al.*, 2012). EO data provide
295 measurements of land surface properties at global scale, allowing the assessment of
296 vegetation dynamics directly (Liu *et al.*, 2015, Nemani *et al.*, 2003) and has also been
297 coupled/compared with vegetation models (Calvet *et al.*, 2004, Poulter *et al.*, 2014). Yet, the
298 most widely used EO data for EO/DGVM fusion is the optical satellite sensor vegetation
299 index observations (NDVI) which are shown here to be unrelated to the non-photosynthetic
300 woody vegetation component. This might be one of the reasons for the large discrepancy
301 between the global terrestrial carbon storage estimated from DGVMs and EO data,
302 respectively (Kolby Smith *et al.*, 2016). Therefore, if aiming at improved assessment of e.g.
303 changes in dryland carbon pools or woody vegetation cover/mass changes (from EO data
304 alone or assimilated into DGVMs), the presented method of combining EO optical and
305 microwave remote sensing is expected to outperform the use of each of them separately.

306 ***Interpretation of sub-continental hot-spot regions of VOD_{wood} change***

307 The areas of increasing VOD_{wood} trends in Mexico and Texas, USA are likely related to shrub
308 encroachment mainly happening in the Chihuahuan Desert (Aide *et al.*, 2013, Van Auken,
309 2009), which was reported to be accelerating caused by a changing climatic conditions of
310 increasing temperatures (D'Odorico *et al.*, 2010). The significant decreasing VOD_{wood} trend in
311 the southeast of Texas corresponds well with the 2011 drought causing large scale tree
312 mortality as reported by Schwantes *et al.* (2016).

313 Extensive deforestation has taken place in vast parts of the Gran Chaco region characterized
314 by a transformation from dry deciduous forest into agriculture land (soybean production)
315 (Gasparri & Grau, 2009). These changes in land cover and land use (LULCC) were also
316 captured by medium/high resolution Landsat data (Hansen *et al.*, 2013). The VOD_{wood} trend
317 successfully detected this LULCC as a pronounced and widespread woody vegetation loss.

318 A return of woody vegetation in the Brazilian Caatinga region caused by the increases in
319 rainfall and decrease in the area under cultivation during 2001-2009 was reported by Redo *et*
320 *al.* (2013), which may explain the strongly positive VOD_{wood} trends in our analysis in
321 northeast part of Brazil. Contrastingly, decreasing VOD_{wood} trends in the south of Brazil
322 indicating a loss of woody vegetation, are likely to be caused by the highly degraded soil
323 conditions in this region (Almeida-Filho & Carvalho, 2010).

324 In the African Sahel, a greening trend driven by increasing rainfall after prolonged droughts
325 was reported using the AVHRR NDVI datasets (Herrmann *et al.*, 2005, Prince *et al.*, 2007).
326 However, this greening trend starting from early 1980s seems to have stabilized as assessed
327 using data from the MODIS sensor since 2000 (Horion *et al.*, 2014). This agrees well with the
328 NDVI based leaf component trend in this study (Fig. 3b). The widespread significant positive
329 VOD_{wood} trends (Fig. 6d) indicate that the density of woody vegetation stands have continued

330 to increase during 2000-2012, which is in line with the findings of Brandt *et al.* (2016a).
331 Besides the overall increasing trend, losses of woody vegetation are also seen in the Sahel e.g.
332 northern Nigeria which was reported to be caused by logging and agricultural expansion into
333 forest reserves (Brandt *et al.*, 2016a).

334 The extensive shrub encroachment in the drylands of Namibia and South Africa (Buitenwerf
335 *et al.*, 2012, O'Connor *et al.*, 2014, Rohde & Hoffman, 2012) is supported by the significant
336 positive trends in both the NDVI based leaf component and retrieved VOD_{wood} based woody
337 component. However, the VOD_{wood} shows much larger areas of positive trends as compared to
338 NDVI (Fig. 4), indicating a potential under-estimation of the spatial extent of shrub
339 encroachment based on optical remote sensing data in this region (Saha *et al.*, 2015).
340 Manmade fires are used for controlling bush encroachment in Botswana and Zimbabwe
341 (Gandiwa, 2011, Mudongo *et al.*, 2016). While fire rarely kill trees, bush encroachment is
342 suppressed and ultimately will lead to a reduction in the size of woody plants (Higgins *et al.*,
343 2007). Therefore, an intensification of fire events during this period as observed by Andela
344 and van der Werf (2014) would be a plausible explanation for the overall decreasing VOD_{wood}
345 trends in Botswana and Zimbabwe.

346 Selective logging of hardwood trees species for charcoal production was reported to introduce
347 land degradation in the woodland regions of Kenya (Ndegwa *et al.*, 2016). Also, massive
348 logging and deforestation for charcoal and livestock production is happening in Somalia
349 (Oduori *et al.*, 2011, Rembold *et al.*, 2013) which together may explain the widespread
350 pattern of decreasing VOD_{wood} trends in East Africa (Fig. 6f).

351 A consistent increasing trend was observed in the retrieved VOD_{wood} for India, meaning an
352 increase in the forest cover or natural growth of trees during the period studied. This may be

353 attributed to the large scale implementation of policies aiming at developing forest protection
354 programs (Reddy *et al.*, 2013, Tian *et al.*, 2014).

355 The geographical patterns of VOD_{wood} trends in Australia correspond well with the substantial
356 changes in water availability during the period studied (Xie *et al.*, 2016). A continues decline
357 in water storage was reported in Australia during the early 21st-century caused by long lasting
358 droughts (known as the ‘big dry’), being particularly severe in the southwestern part causing
359 widespread tree mortality (Brouwers *et al.*, 2013, McGrath *et al.*, 2012). Effects of water loss
360 were compensated or even reversed by a continental-scale water gain in 2010 and 2011,
361 particularly strong in the eastern part (Xie *et al.*, 2016).

362 ***Limitations and Outlook***

363 The microwave observations used in this long-term VOD dataset cannot always penetrate the
364 entire vegetation layer (e.g. rainforest). To mitigate this potential limitation of the usage of
365 VOD, our study focuses on dryland areas only. Since we are aiming to detect changes in the
366 woody component, herbaceous and crops would perturb the estimation accuracy due to their
367 different relationships with satellite observations as compared to woody vegetation (Tian *et*
368 *al.*, 2016). The use of VOD observations from only the dry season facilitates accurate
369 detection of the water content in woody component, but remnants of senescent material from
370 leftover herbaceous vegetation and crops, together with soil background, may still introduce
371 noise. However, a significant relationship between VOD and NDVI time series would ensure
372 that the impacts of error sources on the estimated trends remain at a low level.

373 VOD is reported to be linearly related to the vegetation water content in green vegetation
374 component, depending on vegetation structure, microwave frequency, and vegetation water
375 status (Griend & Wigneron, 2004, Jackson & Schmugge, 1991, Wigneron *et al.*, 2004). Yet,
376 the relationship between VOD and vegetation water content in the woody component may be

377 more complex considering the varying sizes, heights, shapes and species of woody plants
378 (Jones *et al.*, 2011). Furthermore, the relationship between water content/VOD and woody
379 biomass is also expected to be more complex, which may change with the soil conditions and
380 woody species composition (Sternberg & Shoshany, 2001). In combination with a lack of
381 ground observations, these potentially confounding factors made it difficult to transform
382 VOD_{wood} to the units of biomass.

383 The AVHRR sensors have observations since early 1980s, forming the basis for global long-
384 term NDVI datasets. Yet, several problems made it challenging to merge observations from
385 difference sensors in a temporally consistent way (Tian *et al.*, 2015), especially during the dry
386 season (Horion *et al.*, 2014). As for the passive microwave records, although differences of
387 the microwave frequencies exist between sensors (e.g. 19.4 GHz for SSM/I and 6.9GHz for
388 AMSR-E), the sensitivity of observed microwave emissions to the leaf component was
389 reported to be similar at these frequencies (Santi *et al.*, 2009). Moreover, the long overlapping
390 period between different sensors made it possible to calibrate VOD retrievals successfully
391 (Liu *et al.*, 2011). Consequently, the availability of an improved AVHRR based long-term
392 NDVI products (expected release in the near future) will extend the analysis period of woody
393 component trends to around three decades.

394 Recently, several passive microwave satellite instruments operating at L-band (1.4 GHz) have
395 been launched, i.e. the Soil Moisture and Ocean Salinity (SMOS, 2010 - present), the
396 Aquarius (2011 - 2015) and the Soil Moisture Active Passive (SMAP). As the leaf component
397 is close to be transparent at L-band (Guglielmetti *et al.*, 2007, Santi *et al.*, 2009), observations
398 from these sensors are expected to be more directly linked to information on the woody
399 component (Grant *et al.*, 2016, Vittucci *et al.*, 2016). Due to their short time period of
400 operation, trend analyses on these L-band observations are not yet feasible. However, with

401 observations continued in the near future, temporal trends of VOD retrievals from SMOS and
402 SMAP can be compared with the trends of the approach developed in this study. If promising,
403 they can be merged into a long-term time series to assist analyzing changes in woody
404 vegetation.

405

406 **Acknowledgements**

407 This research is partly funded by the China Scholarship Council (CSC, number
408 201306420005) and the Danish Council for Independent Research (DFR) Sapere Aude
409 programme under the project entitled "Earth Observation based Vegetation productivity and
410 Land Degradation Trends in Global Drylands". M. B. is the recipient of the European Union's
411 Horizon 2020 research and innovation programme under the Marie Skłodowska-Curie grant
412 agreement (project number 656564). Y.Y.L. is the recipient of an Australian Research
413 Council Discovery Early Career Researcher Award (DECRA) Fellowship (project number
414 DE140100200). We thank the Centre de Suivi Ecologique (Senegal) and especially
415 Abdoulaye Wele and Abdoul Aziz Diouf for collecting and providing the field data on woody
416 cover and leaf biomass, and Neha Joshi, University of Copenhagen for helpful discussions on
417 the properties of passive microwave and radar observations.

418

419 **References**

- 420 Adeel Z, Safriel U, Niemeijer D *et al.* (2005) *Ecosystems and human well-being: desertification*
421 *synthesis. A Report of the Millennium Ecosystem Assessment*, Washington, DC, World
422 Resources Institute.
- 423 Ahlstrom A, Raupach MR, Schurgers G *et al.* (2015) The dominant role of semi-arid ecosystems in
424 the trend and variability of the land CO₂ sink. *Science*, **348**, 895-899.
- 425 Aide TM, Clark ML, Grau HR *et al.* (2013) Deforestation and Reforestation of Latin America and the
426 Caribbean (2001–2010). *Biotropica*, **45**, 262-271.

- 427 Almeida-Filho R, Carvalho CM (2010) Mapping land degradation in the Gilbués region, northeastern
428 Brazil, using Landsat TM images. *International Journal of Remote Sensing*, **31**, 1087-1094.
- 429 Andela N, Liu YY, Van Dijk AIJM, De Jeu RaM, Mcvicar TR (2013) Global changes in dryland
430 vegetation dynamics (1988-2008) assessed by satellite remote sensing: comparing a new
431 passive microwave vegetation density record with reflective greenness data. *Biogeosciences*,
432 **10**, 6657-6676.
- 433 Andela N, Van Der Werf GR (2014) Recent trends in African fires driven by cropland expansion and
434 El Nino to La Nina transition. *Nature Climate Change*, **4**, 791-795.
- 435 Archibald S, Scholes RJ (2007) Leaf green-up in a semi-arid African savanna -separating tree and
436 grass responses to environmental cues. *Journal of Vegetation Science*, **18**, 583-594.
- 437 Brandt M, Hiernaux P, Rasmussen K *et al.* (2016a) Assessing woody vegetation trends in Sahelian
438 drylands using MODIS based seasonal metrics. *Remote Sensing of Environment*, **183**, 215-
439 225.
- 440 Brandt M, Hiernaux P, Tagesson T *et al.* (2016b) Woody plant cover estimation in drylands from
441 Earth Observation based seasonal metrics. *Remote Sensing of Environment*, **172**, 28-38.
- 442 Brandt M, Mbow C, Diouf AA, Verger A, Samimi C, Fensholt R (2015) Ground- and satellite-based
443 evidence of the biophysical mechanisms behind the greening Sahel. *Global Change Biology*,
444 1610-1620.
- 445 Brouwers NC, Mercer J, Lyons T, Poot P, Veneklaas E, Hardy G (2013) Climate and landscape
446 drivers of tree decline in a Mediterranean ecoregion. *Ecology and Evolution*, **3**, 67-79.
- 447 Buitenwerf R, Bond WJ, Stevens N, Trollope WSW (2012) Increased tree densities in South African
448 savannas: >50 years of data suggests CO2 as a driver. *Global Change Biology*, **18**, 675-684.
- 449 Calvet JC, Viterbo P, Ciais P *et al.* (2004) Assimilation of remote sensing data to monitor the
450 terrestrial carbon cycle: The carbon observatory of geoland. In: *Geoscience and Remote
451 Sensing Symposium, 2004. IGARSS '04. Proceedings. 2004 IEEE International*. pp Page.
- 452 D'odorico P, Fuentes JD, Pockman WT *et al.* (2010) Positive feedback between microclimate and
453 shrub encroachment in the northern Chihuahuan desert. *Ecosphere*, **1**, 1-11.
- 454 De Kauwe MG, Medlyn BE, Zaehle S *et al.* (2014) Where does the carbon go? A model–data
455 intercomparison of vegetation carbon allocation and turnover processes at two temperate
456 forest free-air CO2 enrichment sites. *New Phytologist*, **203**, 883-899.
- 457 Detsch F, Otte I, Appelhans T, Nauss T (2016) A Comparative Study of Cross-Product NDVI
458 Dynamics in the Kilimanjaro Region—A Matter of Sensor, Degradation Calibration, and
459 Significance. *Remote Sensing*, **8**, 159.
- 460 Diallo O, Diouf A, Hanan NP, Ndiaye A, Prévost Y (1991) AVHRR monitoring of savanna primary
461 production in Senegal, West Africa: 1987-1988. *International Journal of Remote Sensing*, **12**,
462 1259-1279.
- 463 Didan K (2015) MOD13C2 MODIS/Terra Vegetation Indices Monthly L3 Global 0.05Deg CMG
464 V006. NASA EOSDIS Land Processes DAAC. Retrieved from
465 <http://dx.doi.org/10.5067/MODIS/MOD13C2.006>.
- 466 Diouf A, Brandt M, Verger A *et al.* (2015) Fodder Biomass Monitoring in Sahelian Rangelands Using
467 Phenological Metrics from FAPAR Time Series. *Remote Sensing*, **7**, 9122.
- 468 Donohue RJ, Mcvicar TR, Roderick ML (2009) Climate-related trends in Australian vegetation cover
469 as inferred from satellite observations, 1981–2006. *Global Change Biology*, **15**, 1025-1039.
- 470 Fensholt R, Horion S, Tagesson T, Ehammer A, Ivits E, Rasmussen K (2015) Global-scale mapping of
471 changes in ecosystem functioning from earth observation-based trends in total and recurrent
472 vegetation. *Global Ecology and Biogeography*, **24**, 1003-1017.
- 473 Fensholt R, Langanke T, Rasmussen K *et al.* (2012) Greenness in semi-arid areas across the globe
474 1981–2007 — an Earth Observing Satellite based analysis of trends and drivers. *Remote
475 Sensing of Environment*, **121**, 144-158.
- 476 Fensholt R, Sandholt I, Rasmussen MS, Stisen S, Diouf A (2006) Evaluation of satellite based primary
477 production modelling in the semi-arid Sahel. *Remote Sensing of Environment*, **105**, 173-188.
- 478 Ferrazzoli P, Guerriero L, Wigneron JP (2002) Simulating L-band emission of forests in view of
479 future satellite applications. *Ieee Transactions on Geoscience and Remote Sensing*, **40**, 2700-
480 2708.
- 481 Gandiwa E (2011) Effects of repeated burning on woody vegetation structure and composition in a
482 semiarid southern African savanna. *International journal of environmental sciences*, **2**, 458.
- 483 Gasparri NI, Grau HR (2009) Deforestation and fragmentation of Chaco dry forest in NW Argentina
484 (1972–2007). *Forest Ecology and Management*, **258**, 913-921.

485 Grant JP, Wigneron JP, De Jeu RaM *et al.* (2016) Comparison of SMOS and AMSR-E vegetation
486 optical depth to four MODIS-based vegetation indices. *Remote Sensing of Environment*, **172**,
487 87-100.

488 Griend AaVD, Wigneron JP (2004) The b-factor as a function of frequency and canopy type at H-
489 polarization. *Ieee Transactions on Geoscience and Remote Sensing*, **42**, 786-794.

490 Guglielmetti M, Schwank M, Mätzler C, Oberdörster C, Vanderborcht J, Flübler H (2007) Measured
491 microwave radiative transfer properties of a deciduous forest canopy. *Remote Sensing of*
492 *Environment*, **109**, 523-532.

493 Hansen MC, Potapov PV, Moore R *et al.* (2013) High-Resolution Global Maps of 21st-Century Forest
494 Cover Change. *Science*, **342**, 850-853.

495 Herrmann SM, Anyamba A, Tucker CJ (2005) Recent trends in vegetation dynamics in the African
496 Sahel and their relationship to climate. *Global Environmental Change*, **15**, 394-404.

497 Herrmann SM, Tappan GG (2013) Vegetation impoverishment despite greening: A case study from
498 central Senegal. *Journal of Arid Environments*, **90**, 55-66.

499 Higgins SI, Bond WJ, February EC *et al.* (2007) Effects of four decades of fire manipulation on
500 woody vegetation structure in savanna. *Ecology*, **88**, 1119-1125.

501 Horion S, Fensholt R, Tagesson T, Ehammer A (2014) Using earth observation-based dry season
502 NDVI trends for assessment of changes in tree cover in the Sahel. *International Journal of*
503 *Remote Sensing*, **35**, 2493-2515.

504 Horion S, Prishchepov AV, Verbesselt J, De Beurs K, Tagesson T, Fensholt R (2016) Revealing
505 turning points in ecosystem functioning over the Northern Eurasian agricultural frontier.
506 *Global Change Biology*, n/a-n/a.

507 Huete AR (1988) A soil-adjusted vegetation index (SAVI). *Remote Sensing of Environment*, **25**, 295-
508 309.

509 Ippcc (2014) Climate Change 2014: Synthesis Report. Contribution of Working Groups I, II and III to
510 the Fifth Assessment Report of the Intergovernmental Panel on Climate Change [Core Writing
511 Team, R.K. Pachauri and L.A. Meyer (eds.)]. IPCC, Geneva, Switzerland, 151 pp.

512 Jackson TJ, Schmugge TJ (1991) Vegetation effects on the microwave emission of soils. *Remote*
513 *Sensing of Environment*, **36**, 203-212.

514 Jones MO, Jones LA, Kimball JS, Mcdonald KC (2011) Satellite passive microwave remote sensing
515 for monitoring global land surface phenology. *Remote Sensing of Environment*, **115**, 1102-
516 1114.

517 Jones MO, Kimball JS, Jones LA (2013) Satellite microwave detection of boreal forest recovery from
518 the extreme 2004 wildfires in Alaska and Canada. *Global Change Biology*, **19**, 3111-3122.

519 Kerr YH (2007) Soil moisture from space: Where are we? *Hydrogeology Journal*, **15**, 117-120.

520 Kolby Smith W, Reed SC, Cleveland CC *et al.* (2016) Large divergence of satellite and Earth system
521 model estimates of global terrestrial CO₂ fertilization. *Nature Clim. Change*, **6**, 306-310.

522 Liu YY, De Jeu RaM, Mccabe MF, Evans JP, Van Dijk AIJM (2011) Global long-term passive
523 microwave satellite-based retrievals of vegetation optical depth. *Geophysical Research*
524 *Letters*, **38**.

525 Liu YY, Dorigo WA, Parinussa RM *et al.* (2012) Trend-preserving blending of passive and active
526 microwave soil moisture retrievals. *Remote Sensing of Environment*, **123**, 280-297.

527 Liu YY, Van Dijk AIJM, De Jeu RaM, Canadell JG, Mccabe MF, Evans JP, Wang G (2015) Recent
528 reversal in loss of global terrestrial biomass. *Nature Climate Change*, **5**, 470-474.

529 Lyapustin A, Wang Y, Xiong X *et al.* (2014) Scientific impact of MODIS C5 calibration degradation
530 and C6+ improvements. *Atmospheric Measurement Techniques*, **7**, 4353-4365.

531 Mcgrath GS, Sadler R, Fleming K, Tregoning P, Hinz C, Veneklaas EJ (2012) Tropical cyclones and
532 the ecohydrology of Australia's recent continental-scale drought. *Geophysical Research*
533 *Letters*, **39**, n/a-n/a.

534 Mitchard ETA, Flintrop CM (2013) Woody encroachment and forest degradation in sub-Saharan
535 Africa's woodlands and savannas 1982–2006. *Philosophical Transactions of the Royal Society*
536 *of London B: Biological Sciences*, **368**.

537 Mitchard ETA, Saatchi SS, Woodhouse IH *et al.* (2009) Using satellite radar backscatter to predict
538 above-ground woody biomass: A consistent relationship across four different African
539 landscapes. *Geophysical Research Letters*, **36**, n/a-n/a.

540 Mudongo E, Fynn R, Bonyongo MC (2016) Influence of fire on woody vegetation density, cover and
541 structure at Tiisa Kalahari Ranch in western Botswana. *Grassland Science*, **62**, 3-11.

- 542 Ndegwa GM, Nehren U, Grüninger F, Iiyama M, Anhof D (2016) Charcoal production through
543 selective logging leads to degradation of dry woodlands: a case study from Mutomo District,
544 Kenya. *Journal of Arid Land*, **8**, 618-631.
- 545 Nemani RR, Keeling CD, Hashimoto H *et al.* (2003) Climate-Driven Increases in Global Terrestrial
546 Net Primary Production from 1982 to 1999. *Science*, **300**, 1560-1563.
- 547 O'connor TG, Puttick JR, Hoffman MT (2014) Bush encroachment in southern Africa: changes and
548 causes. *African Journal of Range & Forage Science*, **31**, 67-88.
- 549 Oduori SM, Rembold F, Abdulle OH, Vargas R (2011) Assessment of charcoal driven deforestation
550 rates in a fragile rangeland environment in North Eastern Somalia using very high resolution
551 imagery. *Journal of Arid Environments*, **75**, 1173-1181.
- 552 Owe M, De Jeu R, Walker J (2001) A methodology for surface soil moisture and vegetation optical
553 depth retrieval using the microwave polarization difference index. *Ieee Transactions on*
554 *Geoscience and Remote Sensing*, **39**, 1643-1654.
- 555 Piao S, Sitch S, Ciais P *et al.* (2013) Evaluation of terrestrial carbon cycle models for their response to
556 climate variability and to CO₂ trends. *Global Change Biology*, **19**, 2117-2132.
- 557 Poorter H, Niklas KJ, Reich PB, Oleksyn J, Poot P, Mommer L (2012) Biomass allocation to leaves,
558 stems and roots: meta-analyses of interspecific variation and environmental control. *New*
559 *Phytologist*, **193**, 30-50.
- 560 Poulter B, Frank D, Ciais P *et al.* (2014) Contribution of semi-arid ecosystems to interannual
561 variability of the global carbon cycle. *Nature*, **509**, 600-603.
- 562 Prince SD, Wessels KJ, Tucker CJ, Nicholson SE (2007) Desertification in the Sahel: a
563 reinterpretation of a reinterpretation. *Global Change Biology*, **13**, 1308-1313.
- 564 Reddy CS, Dutta K, Jha CS (2013) Analysing the gross and net deforestation rates in India. *Current*
565 *Science*, **105**, 1492-1500.
- 566 Redo D, Aide TM, Clark ML (2013) Vegetation change in Brazil's dryland ecoregions and the
567 relationship to crop production and environmental factors: Cerrado, Caatinga, and Mato
568 Grosso, 2001–2009. *Journal of Land Use Science*, **8**, 123-153.
- 569 Rembold F, Oduori SM, Gadain H, Toselli P (2013) Mapping charcoal driven forest degradation
570 during the main period of Al Shabaab control in Southern Somalia. *Energy for Sustainable*
571 *Development*, **17**, 510-514.
- 572 Rohde RF, Hoffman MT (2012) The historical ecology of Namibian rangelands: Vegetation change
573 since 1876 in response to local and global drivers. *Science of The Total Environment*, **416**,
574 276-288.
- 575 Saha MV, Scanlon TM, D'odorico P (2015) Examining the linkage between shrub encroachment and
576 recent greening in water-limited southern Africa. *Ecosphere*, **6**, 1-16.
- 577 Santi E, Paloscia S, Pampaloni P, Pettinato S (2009) Ground-Based Microwave Investigations of
578 Forest Plots in Italy. *Ieee Transactions on Geoscience and Remote Sensing*, **47**, 3016-3025.
- 579 Schwantes AM, Swenson JJ, Jackson RB (2016) Quantifying drought-induced tree mortality in the
580 open canopy woodlands of central Texas. *Remote Sensing of Environment*, **181**, 54-64.
- 581 Shimada M, Itoh T, Motooka T, Watanabe M, Shiraishi T, Thapa R, Lucas R (2014) New global
582 forest/non-forest maps from ALOS PALSAR data (2007–2010). *Remote Sensing of*
583 *Environment*, **155**, 13-31.
- 584 Sternberg M, Shoshany M (2001) Aboveground biomass allocation and water content relationships in
585 Mediterranean trees and shrubs in two climatological regions in Israel. *Plant Ecology*, **157**,
586 173-181.
- 587 Tian F, Brandt M, Liu YY *et al.* (2016) Remote sensing of vegetation dynamics in drylands:
588 Evaluating vegetation optical depth (VOD) using AVHRR NDVI and in situ green biomass
589 data over West African Sahel. *Remote Sensing of Environment*, **177**, 265-276.
- 590 Tian F, Fensholt R, Verbesselt J, Grogan K, Horion S, Wang Y (2015) Evaluating temporal
591 consistency of long-term global NDVI datasets for trend analysis. *Remote Sensing of*
592 *Environment*, **163**, 326-340.
- 593 Tian H, Banger K, Bo T, Dadhwal VK (2014) History of land use in India during 1880–2010: Large-
594 scale land transformations reconstructed from satellite data and historical archives. *Global and*
595 *Planetary Change*, **121**, 78-88.
- 596 Van Auken OW (2009) Causes and consequences of woody plant encroachment into western North
597 American grasslands. *Journal of Environmental Management*, **90**, 2931-2942.
- 598 Vermote EF, Kotchenova S (2008) Atmospheric correction for the monitoring of land surfaces.
599 *Journal of Geophysical Research: Atmospheres*, **113**, 1-12.

600 Vittucci C, Ferrazzoli P, Kerr Y, Richaume P, Guerriero L, Rahmoune R, Laurin GV (2016) SMOS
601 retrieval over forests: Exploitation of optical depth and tests of soil moisture estimates.
602 Remote Sensing of Environment, **180**, 115-127.
603 Wigneron J-P, Kerr Y, Chanzy A, Jin Y-Q (1993) Inversion of surface parameters from passive
604 microwave measurements over a soybean field. Remote Sensing of Environment, **46**, 61-72.
605 Wigneron JP, Parde M, Waldteufel P, Chanzy A, Kerr Y, Schmidl S, Skou N (2004) Characterizing
606 the dependence of vegetation model parameters on crop structure, incidence angle, and
607 polarization at L-band. Ieee Transactions on Geoscience and Remote Sensing, **42**, 416-425.
608 Xie Z, Huete A, Restrepo-Coupe N, Ma X, Devadas R, Caprarelli G (2016) Spatial partitioning and
609 temporal evolution of Australia's total water storage under extreme hydroclimatic impacts.
610 Remote Sensing of Environment, **183**, 43-52.

611

612 **Supporting Information captions**

613 **Fig. S1.** Example of the conceptual design based on simulated data.

614 **Fig. S2.** Location of the *in situ* sites.

615 **Fig. S3.** *In situ* measurements of leaf biomass and woody cover data.